

Document downloaded from:

<http://hdl.handle.net/10251/108071>

This paper must be cited as:

Gamiz Gonzalez, MA.; Edlund, U.; Vidaurre, A.; Gómez Ribelles, JL. (2017). Synthesis of highly swellable hydrogels of water-soluble carboxymethyl chitosan and poly(ethylene glycol). *Polymer International*. 66(11):1624-1632. doi:10.1002/pi.5424



The final publication is available at

<https://doi.org/10.1002/pi.5424>

Copyright John Wiley & Sons

Additional Information

# Synthesis of highly swellable hydrogels of water-soluble Carboxymethyl chitosan and Poly(ethylene glycol).

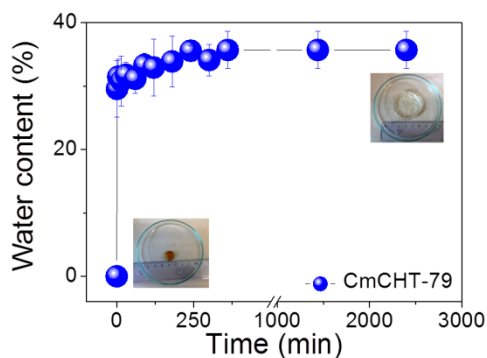
M. A. Gámiz-González<sup>a</sup>, Ulrica Edlund<sup>b</sup>, A. Vidaurre<sup>a,c</sup> and J. L. Gómez Ribelles<sup>a,c</sup>.

<sup>a</sup>Centre for Biomaterials and Tissue Engineering (CBIT), Universitat Politècnica de Valencia, Camino de Vera s/n, 46022, Valencia, Spain

<sup>b</sup>Fibre and Polymer Technology, School of Chemical Science and Engineering, KTH Royal Institute of Technology, SE-100 44, Stockholm, Sweden

<sup>c</sup>Biomedical Research Networking Center in Bioengineering, Biomaterials and Nanomedicine (CIBER-BBN), Spain

## Graphical abstract



Highly swellable hydrogels by cross-linking of carboxymethyl chitosan with poly(ethylene glycol) for CmCHT-79

## Abstract

Highly swellable hydrogels were produced by crosslinking of high molecular weight carboxymethylated chitosan (CmCHT) with poly(ethylene glycol) (PEG) oligomers. The hydrogel swelling capacity could be controlled via the crosslinking density and ranged from 900 to 5600 %.

The hydrogels showed good homogeneity with a high interconnected porosity in the swollen state and with nanodomains rich in CmCHT and others rich in PEGDE. Oscillatory frequency sweep analysis showed a storage modulus of ca 27 kPa for the hydrogel with the highest crosslinking density, which, together with the exhibited enzyme degradability with lysozyme at 59 days indicate that these hydrogels have potential use in delivery systems or soft tissue regeneration.

## Introduction

Chitosan (CHT) is a polymer amenable to chemical modifications. The linear polymer has three reactive groups in its structure; in (C-2) it has the amino group (NH<sub>2</sub>) on each deacetylated unit; it also has hydroxyl groups (OH) in primary (C-3) and secondary (C-6). These reactive groups mean that chitosan can react with different chemical groups to alter its physico-chemical and biological properties.

Carboxymethylchitosan (CmCHT) is obtained from the N,O-carboxymethylation of chitosan. It is an important water-soluble chitosan derivative due to its amphoteric nature [1]. CmCHT has tremendous biomedical potential for use like a drug delivery system or like a carrier matrices systems due to its biocompatibility, biodegradability and immunogenicity.

Syntheses of hydrogels by covalent cross-linking have been carried out on strategies for seeking materials with tunable properties to obtain hydrogels by block-copolymer networks. Chitosan networks and its derivatives can be crosslinked by covalent bonds that can be activated in two ways: by using an external cross-linking agent and between polymers with reactive groups. In the case of chitosan, it can be cross-linked by cross-linking agents as glutaraldehyde [2], genipin [3, 4], epichlorohydrin [5], or with other polymers with specific reactive groups able to crosslink directly or by the use of initiators and catalysts [6], e.g. chitosan cross-linked with hyaluronic acid [7], with collagen [8], or with polyurethane to repair skin defects [9]. Crosslinked CmCHT acts as a hydrogel due to the presence of hydrophilic groups that enables the absorption of a large amount of water. The CmCHT hydrogels has been investigated recently for tissue engineering, cartilage regeneration, or as cell-seeded microcarriers [10], in wound dressing and ophthalmic applications [11].

The Poly(ethylene glycol), PEG is a synthetic polyester. The solubility of Poly(ethylene glycol), PEG in water and a wide range of organic solvents in combination with terminal hydroxyl groups are key factors in the successful use to produce PEG block copolymers networks. [12]. PEG [13] is also a good candidate for drug delivery systems [14] or cell delivery systems for various types of cells [15-18]. Williams *et al.*, synthesized photoencapsulated acrylated PEG with mesenchymal stem cells (MSCs) to produce chondrogenesis in vitro [19]. Poon *et al.*, synthesized hydrogels based on dual curable chitosan-graft-poly(ethylene glycol) to cell encapsulation [20].

PEG-based amphiphilic biodegradable hydrogels have been produced by combining PEG with biodegradable hydrophobic polymers such as PLLA, PLGA and PCL [21, 22]. Such

hydrogels present good mechanical properties with moderate hydrolytic degradation rates and water uptake [22]. PEG can also be combined with hydrophilic polymers presenting high water content, such as chitin, chitosan, and collagen[23].

The crosslinking mechanism between CmCHT-PEG polymers was activated via epoxy-amine [24] and via epoxy-hydroxyl reactions [25]. The reactivity of epoxy groups with amino, hydroxyl, and carboxyl groups has been widely used in developing polymer networks [26, 27].

Our aim was to synthesize swellable CmCHT-PEG hydrogels by covalent cross-linking of poly(ethylene glycol) with terminal epoxy groups, the poly(ethylene glycol) diglycidyl ether (PEGDE). FTIR and mechanical testing were also carried out in order to characterize the chemical crosslinking and elastic properties using a rheometer. The macroporous structure of the lyophilized swollen hydrogels obtained from different molar ratio of CmCHT:PEGDE was analyzed by scanning electron microscopy (SEM). In addition, we also have evaluated the enzymatic degradation of the CmCHT-PEG hydrogels with lysozyme.

## **Materials and methods**

### **Materials**

Poly(ethylene glycol) diglycidyl ether (PEGDE) with low molecular weight ( $M_w = 500 \text{ g mol}^{-1}$ ) and sodium hydroxide (NaOH) were purchased from Sigma Aldrich. Carboxymethyl chitosan (CmCHT) with a deacetylation degree (DD) around 90% was obtained from Santa Cruz Biotechnology. The CmCHT was used as received without any further purification. The degree of substitution (DS) was analyzed by a potentiometric method [28] and was found to be  $1.22 \pm 0.04$  carboxymethyl groups per monomeric unit.

### **Methods**

#### **Synthesis of CmCHT-PEG hydrogels**

A series of CmCHT hydrogels was prepared by crosslinking reactions between CmCHT and PEGDE. First, a CmCHT solution in NaOH 1.5M (5%w/v) was prepared: low molecular weight PEGDE (which is a liquid) was added to the CmCHT solution drop by drop. The PEGDE was added in a molar ratio 1:1, 2:1, 7:1 and 10:1 respect to monomeric unit of CmCHT. The initial mass fraction of the PEGDE ( $X_{\text{PEGDE}}$ ) in each hydrogel is

indicated in Table 1. The solution was homogenized by stirring for 30 min and then cured in an oven at 60°C until the solvent was fully evaporated (12 h). The hydrogels were removed from the glass vial and washed several times with deionized water until neutral pH. The samples were freeze-dried at -20°C for 24 h and lyophilized for 48 h obtaining dry porous samples. The porous hydrogels were stored in desiccators under vacuum.

### **Size Exclusion Chromatography (SEC)**

CmCHT molecular weight was measured by SEC on a Dionex Ultimate-3000 HPLC system (Dionex, Sunnyvale, CA, USA), consisting of three PSS Suprema columns in series (300×8 mm, 10 µm particle size) with 30 Å, 100 Å and 1000 Å pore sizes, together with a guard column (50×8 mm, 10 µm particle size). The system was equipped with a WPS-3000SL autosampler, an LPG-3400SD gradient pump, a DAD-3000 UV/Vis detector (Dionex, Sunnyvale, CA, USA) and a Waters-410 refractive index detector (Waters, Millford, MA, USA). Pullulan standards with controlled molecular weights ranging from 342 to 708,000 g mol<sup>-1</sup> (PSS, Germany) were used for calibration [29]. The obtained molecular weight of CmCHT was MW=677 kDa with dispersity index  $\bar{D} = 2.64$ .

### **Scanning Electron Microscopy (SEM)**

The morphology of the porous hydrogels obtained by lyophilization was characterized by a JSM 5410 Scanning Electron Microscope (JOEL, Ltd., Tokyo, Japan), at a working distance of 15 mm and working voltage of 10-15 kV. Samples were fractured after freezing in liquid nitrogen and sputter-coated with gold prior to analysis.

### **Attenuated total reflectance-Fourier transform infrared spectroscopy, (ATR-FTIR)**

ATR-FTIR measurements were performed on a Perkin–Elmer Spectrum 2000 equipped with an attenuated total reflectance (ATR) crystal accessory, within a range of 4000 cm<sup>-1</sup> to 600 cm<sup>-1</sup>. A mean of 16 scans at 4 cm<sup>-1</sup> resolution with atmospheric water and carbon dioxide correction on each sample was recorded and evaluated by the Perkin–Elmer Spectrum software.

### **Water content**

The water content of the samples was evaluated as a function of immersion time. The lyophilized samples (N=5 replicates) between 10-15 mg were immersed in 10 ml of deionized water. To properly measure the water content, the hydrogels were placed in

stainless steel baskets with a mesh opening of 0.20 mm and an inner diameter of 30 mm. The basket was carefully dried for each measurement and the water content (WC) was calculated by Eq(1), where  $m_o$  refers to the dry weight sample and  $m_t$  is the weight of the sample in the swollen state.

$$WC(\%) = \frac{m_t - m_o}{m_o} 100 \quad (1)$$

Moreover, the equilibrium water content, EWC was also obtained as the quantity of water per mass of dry composition once the equilibrium was reached.

### **Thermogravimetric analysis (TGA)**

TGA measurements were performed on a TA-Instrument Model SDT-Q600 system. TGA tests were carried out in alumina crucibles in which samples of weight between 5 and 10 mg were heated from 30 °C to 800 °C at a heating rate of 10° C/min. TGA experiments were performed using a nitrogen flow of 20 mL/min, in order to avoid thermoxidative reduction.

The CmCHT proportion in the polymer network was determined by TGA from the residues obtained at 600°C,  $RW_{600}$ , excluding the water loss in the samples (residue measured at 180°C,  $RW_{180}$ ). Thus, the weight residue of the network,  $RW_{network}$ , was calculated by applying Eq (2):

$$RW_{network} = \frac{RW_{600}}{RW_{180}} 100 \quad (2)$$

The mass fraction of CmCHT,  $X_{CmCHT}$ , and PEGDE,  $X_{PEGDE}$  ( $X_{CmCHT} + X_{PEGDE} = 1$ ) were calculated by applying Eq (3),

$$RW_{network} = (X_{CmCHT} RW_{CmCHT} + X_{PEGDE} RW_{PEGDE})100 \quad (3)$$

Where  $RW_{CmCHT}$  and  $RW_{PEGDE}$  are the CmCHT and PEGDE residues obtained by applying Eq (2) to the pure components.

### **Differential scanning calorimetry (DSC)**

DSC was performed in a Pyris DSC8000 from TA Instruments calibrated with indium and zinc standards in a nitrogen atmosphere. The dry samples (2-10 mg in weight) were kept at 30 °C for 1 min. They were then cooled from 30 to -87 °C at a cooling rate of - 20 °C/min, kept at -87 °C for 2 min and heated from -87 to 90 °C at a heating rate of 20

°C /min, kept at 90°C for 1 min and cooled and heated again under the same conditions. The final temperature was 30 °C.

### **Rheological measurements**

The mechanical properties of CmCMT-PEG hydrogels (N=5 replicates) were evaluated using a parallel plate rheometer, ARES-G2 Rheometer (TA instruments). The hydrogel samples, discs of diameter 8 mm, were swollen in deionized water and carefully transferred to the bottom plate of the rheometer. The experiments were carried out at room temperature (25°C). The gap between the plates was adjusted using a normal force of 0.1 N. Two different measurements in shear deformation mode were performed: for the frequency sweep test the dynamic modulus ( $G'$ ) and loss modulus ( $G''$ ) were evaluated at 1% shear strain amplitude at frequencies ranging from 0.1 to 10 Hz. For the strain sweep tests the module was evaluated at shear strains ranging from 0.1 to 10% at 1 Hz.

### **Enzymatic degradation**

Samples with 5 mm diameter (N=5 replicates for each degradation time) were degraded under enzymatic conditions. The hydrogels were immersed in the enzymatic degradation media, which was prepared by adding 1mg/mL of lysozyme to phosphate buffer solution, PBS (pH=7.4) with 0.02% (w/v) of sodium azide[4]. The temperature was held at 37 °C during the degradation experiments and the degradation media was replaced twice a week. At predefined degradation intervals, the samples were extracted from the degradation media, carefully dried with filter paper and weighed to determine the equilibrium water content by Eq(1). The degraded hydrogels were frozen at -20 °C for 12 h and lyophilized for 24 h. The percentage of the remaining weight after degradation was determined by comparing the weight of the dry sample before degradation ( $m_o$ ) with the weight of the dry sample ( $m_d$ ) using Eq(4):

$$\text{Remaining weight (\%)} = \frac{m_d}{m_o} 100 \quad (4)$$

### **Sample disinfection and indirect cytotoxicity assay**

The hydrogels were disinfected with fungicides and broad-spectrum antibiotics treatment (several washes with deionized sterile water, 100 µg/mL of fungizone antimycotic (Fisher, Spain), 50 µg/mL of ampicilline (Sigma Aldrich, Spain) and 1% penicillin/streptomycin (P/S) (Gibco, UK), dissolution[30].

Sample cytotoxicity was assessed using protocols adapted from the ISO 10993-5 normative. Polystyrene and latex, both sterilized with steam, were selected as a negative control and as positive control respectively. Samples were weighed and cut following the guidelines of ISO 10993-12 previous to immerse in supplemented DMEM without phenol red for 24 hours at 37°C. Cytotoxicity was assessed with L-929 murine fibroblasts that were expanded with DMEM supplemented with 10% of FBS and 1% of P/S and seeded at 10000 cells/well in a 96 well plate. Material liquid extract was added 24 hours after cell seeding. Cell viability was measured 24 hours after initiate the non-contact assay. MTT solution at 10% in DMEM media without phenol red was added and incubated 2.5 hours at 37°C. MTT solution was removed and precipitated salts were dissolved in Nonidet at 0.1% in isopropanol with 4mM of HCl solution. Well plate was read at 570nm.

### **Statistics**

The equilibrium water content was analyzed by ANOVA using SPSS Statistics 16.0 software, while means were compared by the Tukey-*b* test with the level of significance set at  $P < 0.05$ . The results were presented as the mean  $\pm$  standard deviation.

### **Results and discussion**

Highly swellable hydrogels of carboxymethyl chitosan and poly(ethylene glycol) diglycidyl ether were here synthesized through covalent cross-linking of amine, hydroxyl and epoxy groups by ring-opening polymerization.

#### **Synthesis of CmCHT-PEG hydrogels**

The reaction mechanism is schematically shown in Figure 1 and the result of the cross-linking reaction is a block copolymer network containing CmCHT and PEG blocks bonded with -C-N- (amine) and -C-O- (ether) linkages. The time (12 h) and temperature (60 °C) of the preparation process was the same for all compositions, inspired by [31]. The CmCHT 5% (w/v) solution in NaOH 1.5 M showed a yellowish color with a pH around 11. The difference of color of the CmCHT solution dissolved in water (clear solution) and basic (yellowish solution) media was attributed to the possible deacetylation mechanism in the CmCHT polymer in analogy with how chitosan with different degrees of deacetylation (DD) can be obtained from chitin in alkaline media [32]. Deacetylation has also been observed in the synthesis of O-acetyl-galactoglucomannan hydrogels cross-



linked with epichlorohydrin in basic media. The colored solution changed as a function of pH [33].

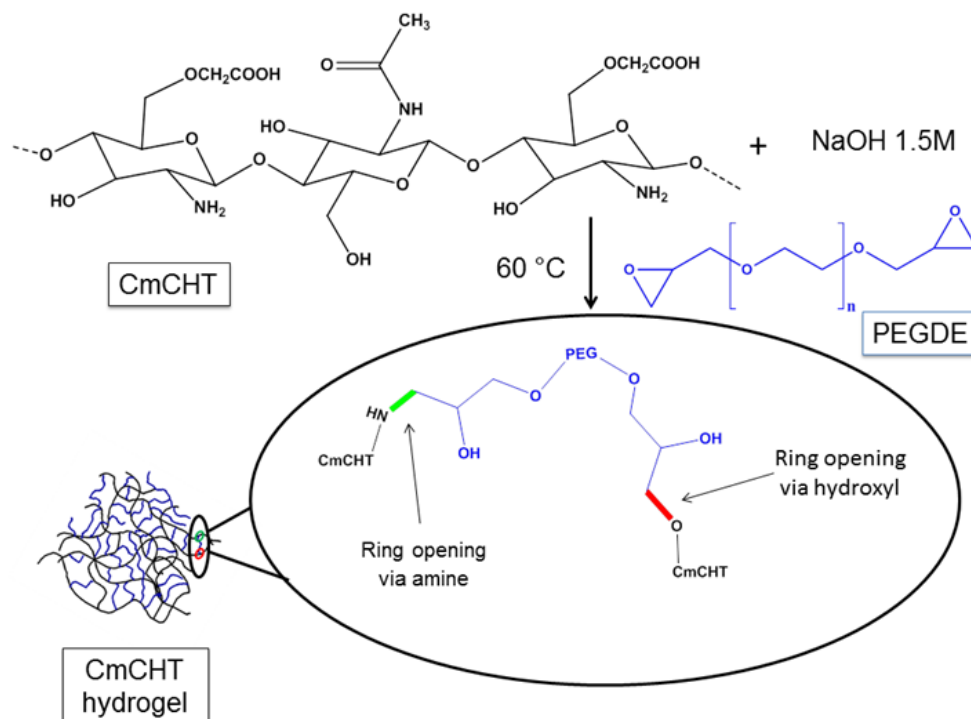


*Figure 1. Scheme of the crosslinking reaction by ring opening via amine and hydroxyl groups from CmCHT polymer. Schematic illustration of the formation of the CmCHT-PEG hydrogel from CmCHT and PEGDE (bottom).*

When PEGDE was added drop by drop under stirring the solution became translucent, indicating a certain degree of liquid-liquid phase separation. Pale yellow hydrogels were obtained, removed from the glass vials, and washed in water several times until neutral pH, verifying that the pale yellow color had disappeared. The samples were frozen and lyophilized.

The final composition of the network was poorly controlled by the amount of PEGDE, as shown in Table 1, but it was possible to obtain a series of block copolymer networks with varying CmCHT content. The Phase separation occurred during the incorporation of PEG blocks to the formed block-copolymer network explains the relatively low PEG content of the resulting material, in spite of the large amount of PEGDE added to the reacting solution. The composition of the resulting network leads to the conclusion that for most of the compositions the hydrogel is formed in the CmCHT-rich phase, while the PEGDE-rich phase is extracted when washing after reaction. Hydrogels were obtained only when PEGDE/CmCHT mass ratio was higher than 75/25. Below this ratio the gel formed could

not be handled due to the low crosslinking density. Interestingly, at very high PEGDE contents a hydrogel rich in PEG blocks can be obtained, so CmCMT-5 contains just 5% CmCMT. In this case, the cross-linking reaction seems to have taken place in the PEGDE-rich phase with CmCMT acting as cross-linker.

*Table 1. Initial and final mass fraction of PEGDE and sample identification for each synthesized hydrogel of CmCMT-PEG.*

<b>Initial mass fraction of PEGDE (<math>X_{PEGDE}</math>)</b>	<b>Final mass fraction of PEGDE analyzed by TGA data</b>	<b>Sample Identification</b>
0.72	0.21	<b>CmCMT-79</b>
0.75	0.11	<b>CmCMT-89</b>
0.94	0.42	<b>CmCMT-58</b>
0.96	0.95	<b>CmCMT-5</b>

Except for the sample with  $X_{PEGDE} = 0.96$  PEGDE starting mass fraction, a low mass fraction of PEGDE remained in the hydrogels, indicating that the covalent crosslinking between PEGDE and CmCMT polymers has a low reactivity (see Table 1). The mass fractions of CmCMT and PEG blocks in the produced hydrogels were estimated by TGA. The yield of the reaction as a function of composition was calculated as the mass of the hydrogel obtained ( $m_{CmCMT-PEG}$ ) with respect to the sum of the initial mass of both polymers ( $m_{CmCMT} + m_{PEGDE}$ ). The values were estimated to  $11 \pm 1$ ,  $20 \pm 7$ ,  $24 \pm 13$  and  $63 \pm 1$  % for CmCMT-89, CmCMT-79, CmCMT-58 and CmCMT-5, respectively, which corroborates our explanation of the mechanism of phase separation given above and that has as a consequence a very low control of the hydrogel composition which does not correlate with the feed ratio of PEGDE.

The curing process in epoxy polymers is influenced by the treatment temperature and polymer concentration. In this synthesis, the temperature and polysaccharide concentrations were chosen based on a literature procedure [34] to obtain hydrogels from carboxymethyl cellulose (CMC) and PEGDE in which was obtained a higher yield than with our CmCMT-PEG hydrogels. This behavior can be attributed to a certain degree of liquid-liquid phase separation, as explained above, as well as the low reactivity between both polymers. The main difference between CMC and CmCMT with respect to this

cross-linking reaction is the reactive groups in the polymer backbone. Whereas CmCMT have amine, hydroxyl and carboxylic reactive groups, CMC have hydroxyl and carboxylic groups. In basic media the amine groups are less reactive than the hydroxyl groups [35]. Due to the N,O- carboxymethyl substitution of the CmCMT [1, 36] the polymer would not have enough free hydroxyl groups to react with the PEGDE epoxy groups.

### Structural analysis of the hydrogels

ATR-FTIR was used to analyze the structural composition of the hydrogels (see Figure 2), which were compared with pristine CmCMT and the PEGDE polymer. A variation between the O-H and N-H stretching peaks appeared, due to the crosslinking between CmCMT and PEGDE. In the reaction new hydroxyl groups appear due to the epoxy ring opening and a broader peak in the 3200-3500  $\text{cm}^{-1}$  region appears when the PEGDE content of the hydrogel is increased.

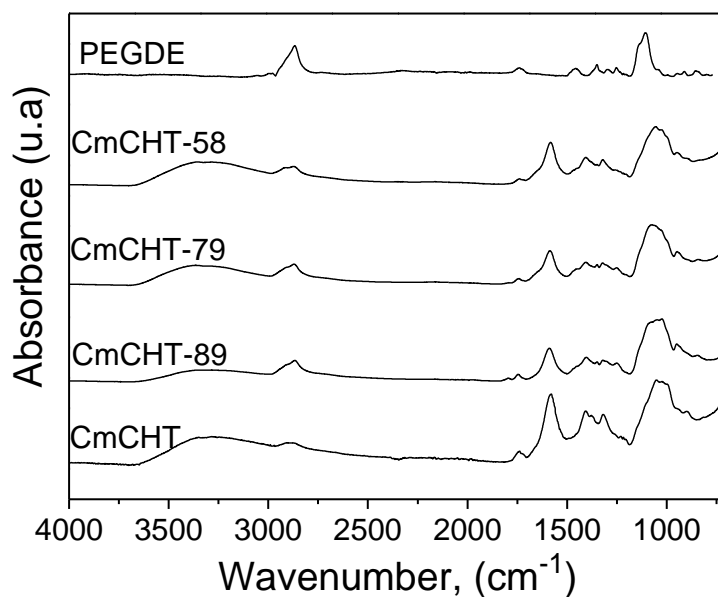


Figure 2. ATR-FTIR spectra of CmCMT -PEG hydrogels and pristine CmCMT and PEGDE.

The new amine bonding appears in the 1244-1246  $\text{cm}^{-1}$  range as a result of the crosslinking due to the opening of the epoxy ring via amine from CmCMT. The crosslinking between the CmCMT hydroxyl groups and the epoxy group can also be observed by the signal that appears at 1036  $\text{cm}^{-1}$  and also the broad peak that appears between 1173 and 868  $\text{cm}^{-1}$ , attributed to ether linkages between hydroxyl groups and

epoxy rings. At  $1741\text{ cm}^{-1}$ , corresponding to the  $-\text{COOH}$  group of the CmCMT polymer, there were no changes between the different hydrogel compositions, indicating that this group is not involved in the reaction [37].

### Hydrogel swelling

Water content for the prepared hydrogels as a function of the immersion time is shown in Figure 3. All the hydrogels reached equilibrium before 180 min, except CmCMT-89, which needed 300 min to do so. All the hydrogels presented very high equilibrium water content, EWC, as both components are hydrophilic polymers. Equilibrium water content was seen to increase as the PEGDE fraction decreased. The statistical analysis indicates that there are significant differences between the EWC of CmCMT-89, CmCMT-79 and CmCMT-58, but no significant differences between the EWC of samples CmCMT-58 and CmCMT-5.

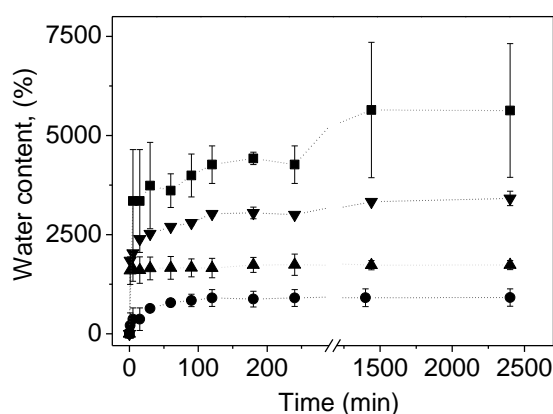


Figure 3. Swelling curves for the CmCMT-PEG hydrogels with different compositions as a function of time, where CmCMT-89(■), CmCMT-79(▼), CmCMT-58 (▲) and CmCMT-5(●).

The results confirm that in addition to having two hydrophilic polymers in the network, crosslinking density is an important factor in determining the water content of the samples. CmCMT-5 equilibrium water content was  $\text{EWC}=900 \pm 200\%$ , whereas the corresponding value for CmCMT-89 was as high as  $\text{EWC}=5600 \pm 1700\%$  mg water with respect to the dry sample.

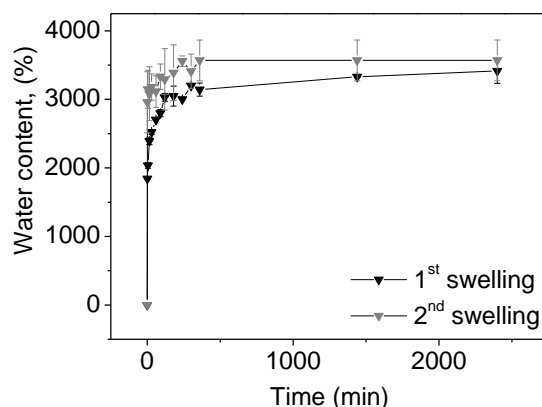


Figure 4. Water content curves of CmCMT-79 hydrogel in two consecutive swelling-drying cycles.

Repeated swelling-deswelling process was carried out to assess the stability of the hydrogel structure. Figure 3 shows two consecutive swelling-cycles of the CmCMT-79 sample in deionized water. Equilibrium water content was  $EWC=3400 \pm 180\%$  after the first swelling and  $EWC=3600 \pm 300\%$  after the second. The samples maintained their shape and dimensions after both swelling cycles, showing that the swelling process is reversible.

### Thermal properties of the hydrogels

The thermal stability of the new hydrogels was studied by TGA and their composition was calculated from the residue measured at  $600^{\circ}\text{C}$ . The thermal decomposition of CmCMT is shown in Figure 5. The first weight loss of around 13%, between  $30-190^{\circ}\text{C}$ , is attributed to water loss. The main degradation step occurs between  $210-310^{\circ}\text{C}$  and a broad shoulder appears around  $317-490^{\circ}\text{C}$ , which is more apparent in the derivative thermogravimetric curve, (DTG) (Figure 5b), where it is resolved as a peak with a maximum around  $T_{\text{max}}=389^{\circ}\text{C}$  which could be ascribed to the thermal degradation of the polymer segments without carboxymethyl substitutions. The range of thermal degradation of CmCMT is below the main thermal degradation of high DD chitosan CHT that takes place between  $200^{\circ}\text{C}-500^{\circ}\text{C}$ , indicating that CmCMT polymer is less thermostable than chitosan [38]. At higher temperatures there is a peak between  $680-766^{\circ}\text{C}$  with a weight loss of around 11%. Miranda *et al.*, [38] observed similar behavior in thermal degradation of CmCMT with a peak around  $602^{\circ}\text{C}$ , which was attributed to the degradation of the residue produced during the previous thermal decomposition.

PEGDE shows a continuous weight loss that could be explained by the loss of short volatile fragments, followed by the main degradation step taking place between 325 and 425°C. The thermal degradation profile of the low molecular weight PEGDE should be different from that of the molecular chains as part of a network. The degradation profile of CmCMT-5 is probably more representative of the PEG blocks of the copolymer network, since those blocks have the chain connectivity of the network and the CmCMT content is low enough to not disturb the interpretation of the thermogram. In this network a single narrow weight step appears centered around 450°C.

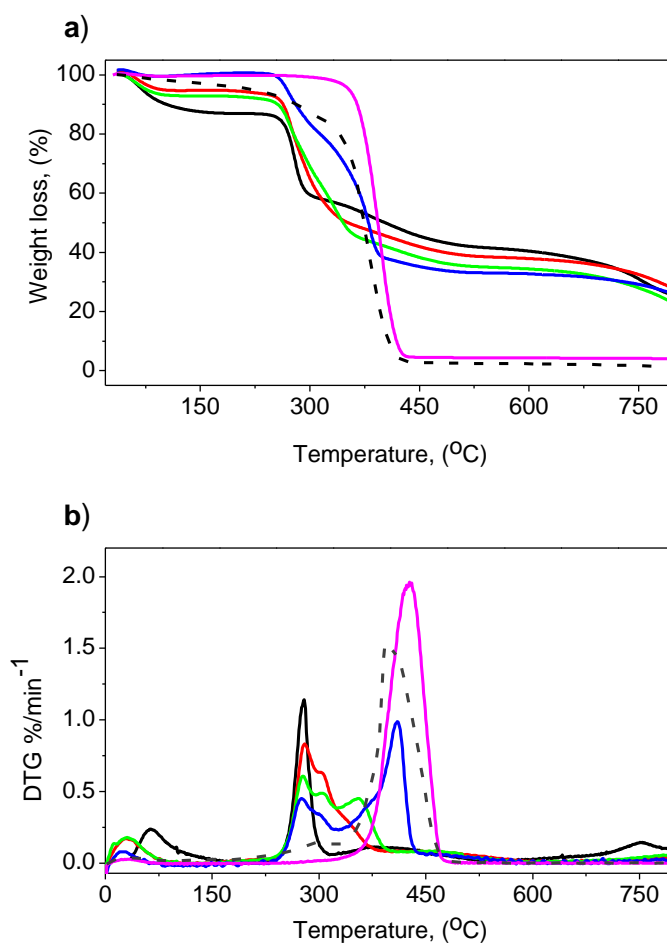


Figure 5.a) TGA and b) DTG curves of CmCMT-PEG hydrogels: CmCMT(-), CmCMT-89(-), CmCMT-79(-), CmCMT-58 (-), CmCMT-5 (-) and PEGDE(---).

The thermal degradation profile of the hydrogels showed the characteristic peaks of the constituent polymers. Nevertheless, a clear shift in the position of the PEG peak towards lower temperatures shows the integration of both components in a single network

structure. For instance, the thermal degradation of the CmCMT-89 presents a  $T_{\text{onset}}=167^{\circ}\text{C}$  until  $T_{\text{end}}=561^{\circ}\text{C}$ , a broad peak that matches with thermal degradation temperature range of pristine polymers, indicating interactions between both polymer chains.

Hydrogel component miscibility was evaluated by DSC. CmCMT did not show either a glass transition or a melting peak in the DSC thermogram. On the other hand, PEGDE presented a broad melting peak in the normalized heat flow curve (Figure 6a) and an exothermal crystallization peak in the normalized cooling thermogram (Figure 6b), with peak temperature  $T_c=-44^{\circ}\text{C}$ . CmCMT-PEG hydrogels did not present any change in the temperature range. This indicates that the distribution of the polymer chains in the network was homogeneous and that phase separation did not take place in the block copolymer network. Unlike pure PEGDE polymer, PEGDE chains cannot reorganize to form crystalline domains in the hydrogel network.

Glass transition temperature was observed in pure PEGDE (Figure 6a), with  $T_{g_{\text{onset}}}=-71^{\circ}\text{C}$ . CmCMT-5 had a higher glass transition temperature ( $T_{g_{\text{onset}}}=-47^{\circ}\text{C}$ ) than pristine PEGDE.

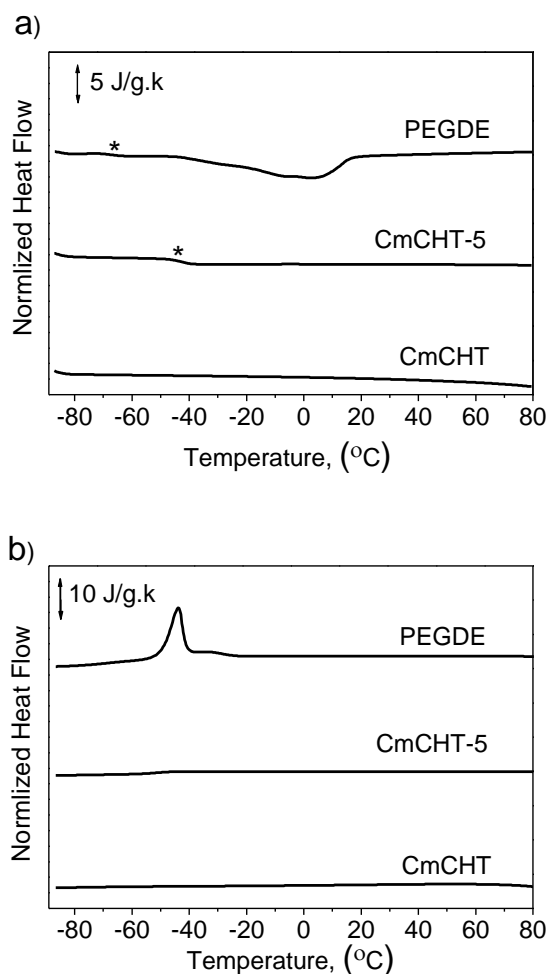


Figure 6. DSC thermograms of the dry hydrogels. a) Second heating scan and b) cooling scan. The symbol \* indicates PEGDE T<sub>g</sub>.

### Rheological properties of the hydrogels

An oscillatory frequency sweep was carried out to determine the mechanical properties of the hydrogels. Measurements of the shear modulus ( $G'$ ) were only possible for CmCHT-79 and CMCHT-58 because the other hydrogel samples were too fragile and disintegrated at the beginning of the test. The  $G'$  values for both samples (Figure 7a) demonstrated that the hydrogel with the highest crosslinking density presented a higher storage modulus value ( $G'=27 \pm 9$  kPa for CmCHT-58 and  $G'=13 \pm 6$  kPa for CmCHT-79 at 1 Hz). No noticeable changes were observed in  $G'$  at all sweep frequencies for any sample. The values of the loss moduli ( $G''$ ) were lower than  $G'$ .



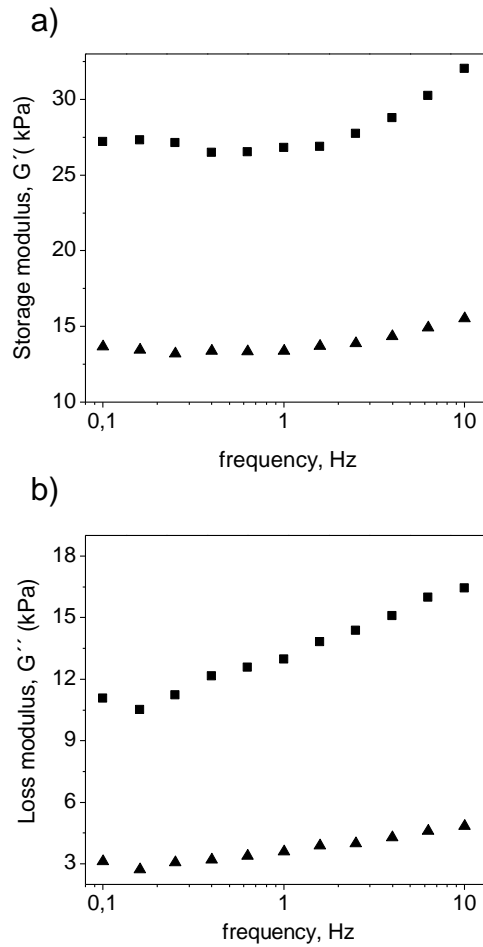


Figure 7. Evolution of a) storage modulus ( $G'$ ) and b) loss moduli, ( $G''$ ) as a function of the frequency for hydrogels CmCHT-79 (▲) and CmCHT-58 (■).

These results suggest that the hydrogels cross-linked with high PEGDE contents are elastic with low viscosity. This behavior was also observed in hydrogels formed by chitosan cross-linked with genipin, but in this case the difference between  $G'$  and  $G''$  was higher than in the CmCHT-PEG hydrogels, with  $G'$  around 100-1000 times higher than  $G''$  [39]. The values of  $G'$  for the hydrogels are in the range of the values used in regeneration of soft tissues [40].

### Morphology of the porous hydrogels

Hydrogels samples were freeze dried from the swollen state to access the macroporous morphology by SEM. The cross-sections of the samples presented an interconnected structure in all the hydrogels. CmCHT-79 presented a laminated structure with pore size

ranging from 160 to 70  $\mu\text{m}$ . The CmCMT-58 hydrogel exhibited a more regular porous structure with a pore size distribution from 40 to 100 $\mu\text{m}$ . As expected, the sample with the highest crosslinking density had a smaller pore size than the sample with the lowest density. The surface of the samples was covered by a thin polymer layer (see cross-section in Figure 8) indicating that some solvent had evaporated from the samples before freezing. This phenomenon has been observed in several honeycomb structures of chitosan hydrogels obtained by the freeze-drying method [41].

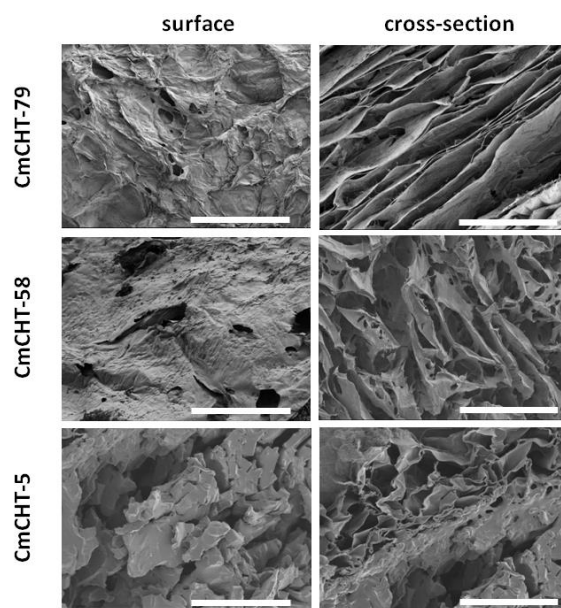


*Figure 8. Surface and cross-section SEM micrographs of hydrogels with different compositions (100x magnification, scale bars represent 600 $\mu\text{m}$ ).*

### **In vitro enzymatic degradation**

The degradation profile of CmCMT-PEGDE samples was tested only in enzymatic conditions for up to 59 days. Other studies have shown that neither CmCMT nor PEG hydrogels had a significant weight loss in a purely hydrolytic medium [42, 43]. The enzymatic degradation profile of the two hydrogels with the highest and lowest content of CmCMT, (CmCMT-89 and CmCMT-5) was analyzed by immersing the samples in a PBS solution containing lysozyme. The remaining weight of the hydrogels was monitored in the degradation process (Figure 9a) for 59 days. Weight loss in both hydrogels was quite small. CmCMT-89 had a remaining weight of  $84 \pm 2\%$  while CmCMT-5 was even less eroded ( $90 \pm 8\%$ ) after 59 days of degradation. Interestingly, enzymatic degradation of the hydrogels produced a sharp increase of equilibrium water content in the first degradation days, (Figure 9b) multiplying the water sorption capacity by a factor of

around 5, while the weight loss is still moderate. The equilibrium water content was calculated applying the Eq(1), where  $m_t$  is the mass weighted at 180 min. The obtained results indicate that the number of effective chains between cross-links decreases, according to Flory-Rehner theory [44]. In the case of CmCMT-89, the EWC (Figure 9b) showed a considerable increase (from 240 % at the beginning of degradation to 25.000 after 14 days of degradation) indicating that the cleavage of chitosan chains had reduced the effective average molecular weight between cross-links. Nevertheless, in the case of CmCMT-5 the increase in equilibrium water content is modest, around  $3800 \pm 900\%$  indicating less cleavage of the PEGDE chains during degradation. After 14 days of degradation the remaining weight was approximately constant for the rest of the time. The evolution of the hydrogel composition as a function of degradation time was calculated by TGA, applying Eq(3). CmCMT-89 presented a higher proportion of CmCMT degradation in the early stages, and the CmCMT fraction fell to 76% after 14 days degradation. The  $X_{CmCMT}$  value did not present any important subsequent changes, (supplementary information (S1)). For CmCMT-5, no significant variations were observed in the mass fraction throughout degradation. In summary, the results from enzymatic degradation of the hydrogels with lysozyme showed that the networks degrade quite slowly, at least during the time span of this study.

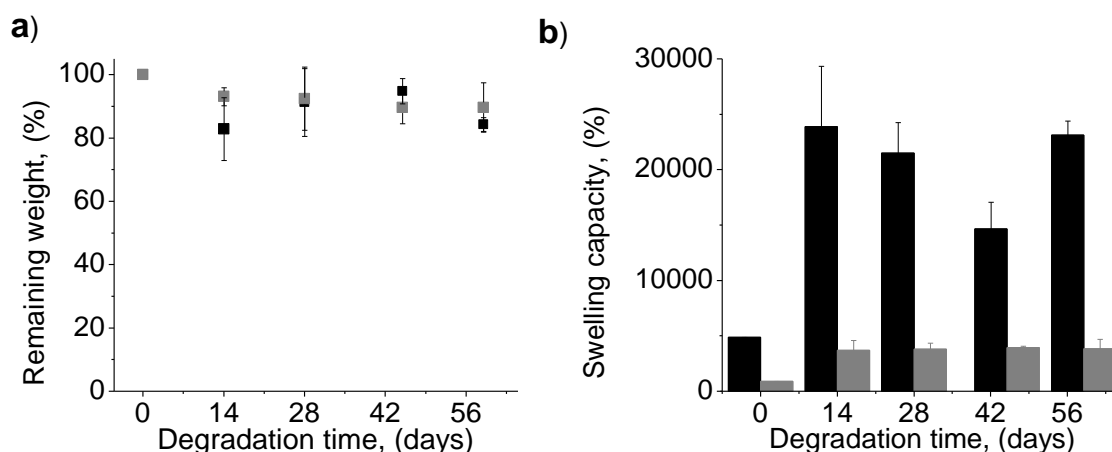


Figure 9. a) Remaining weight of the hydrogels as a function of degradation time during enzymatic degradation and b) water content of both samples CmCMT-89 (■) and CmCMT-5(■).

### Indirect cytotoxicity assay

The cell viability obtained with cytotoxicity assay for CmCMT-PEGDE hydrogels, is

shown in Figure 10. The reference, which relates to cells cultured in polystyrene (C-), was normalized to 100%. It can be observed that all hydrogel compositions present a viability higher than 70% indicating that the material is not cytotoxic.

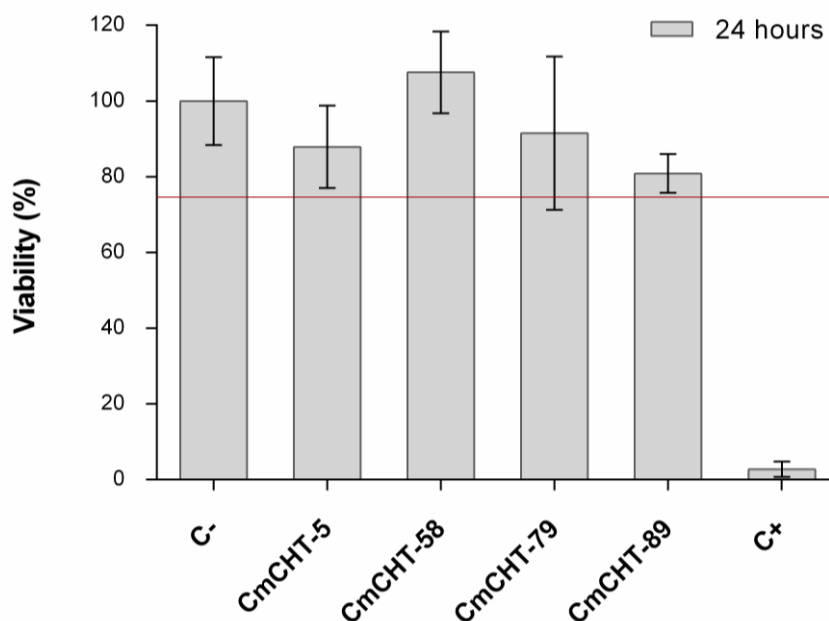


Figure 10. Viability of L-929 murine fibroblasts cultured 24 hours in contact with CmCHT-5, CmCHT- 58, CmCHT-79 and CmCHT-89 hydrogels, latex (C+) and polystyrene (C-). The bars represent the cell viability (%)  $\pm$  standard deviation.

## Conclusions

Block copolymer hydrogel networks were synthesized from CmCHT and PEG with a large swelling capacity (up to 5000%) The crosslinking reaction occurred primarily between the PEGDE epoxy groups and the amine and hydroxyl groups of CmCHT. Covalent crosslinking was confirmed by swelling studies and ATR-FTIR analysis. A double swelling-deswelling process confirmed the stability of the hydrogels even at a low crosslinking density. The mass fraction calculated by the residue measured at 600 °C confirmed that a small fraction of PEGDE was incorporated into the network, which can be explained by a certain degree of immiscibility of the PEGDE and CmCHT in the reacting solution. The rheological measurements showed that these hydrogels are possible candidates for soft material applications. Thermal analysis indicated that both polymers

were homogeneously distributed with no phase separation, as the PEGDE chains were not able to crystallize even in the sample with the highest PEGDE content.

The enzymatic degradation profile of the hydrogels showed a small weight loss in the networks during 59 days of degradation. The cleavage of the CmCHT blocks by lysozyme was detected by an increased swelling capacity of the gels.

## References

- [1] V. Mourya, N. N. Inamdar, and A. Tiwari, "Carboxymethyl chitosan and its applications," *Adv Mat Lett*, vol. 1, pp. 11-33, 2010.
- [2] I. Migneault, C. Dartiguenave, M. J. Bertrand, and K. C. Waldron, "Glutaraldehyde: behavior in aqueous solution, reaction with proteins, and application to enzyme crosslinking," *Biotechniques*, vol. 37, pp. 790-806, 2004.
- [3] F. L. Mi, H. W. Sung, and S. S. Shyu, "Synthesis and characterization of a novel chitosan-based network prepared using naturally occurring crosslinker," *Journal of Polymer Science Part A: Polymer Chemistry*, vol. 38, pp. 2804-2814, 2000.
- [4] F.-L. Mi, Y.-C. Tan, H.-C. Liang, R.-N. Huang, and H.-W. Sung, "In vitro evaluation of a chitosan membrane cross-linked with genipin," *Journal of Biomaterials Science, Polymer Edition*, vol. 12, pp. 835-850, 2001.
- [5] M. Sahin, N. Kocak, G. Arslan, and H. I. Ucan, "Synthesis of crosslinked chitosan with epichlorohydrin possessing two novel polymeric ligands and its use in metal removal," *Journal of Inorganic and Organometallic Polymers and Materials*, vol. 21, pp. 69-80, 2011.
- [6] Y. Hong, Z. Mao, H. Wang, C. Gao, and J. Shen, "Covalently crosslinked chitosan hydrogel formed at neutral pH and body temperature," *Journal of Biomedical Materials Research Part A*, vol. 79, pp. 913-922, 2006.
- [7] L. Li, N. Wang, X. Jin, R. Deng, S. Nie, L. Sun, *et al.*, "Biodegradable and injectable in situ cross-linking chitosan-hyaluronic acid based hydrogels for postoperative adhesion prevention," *Biomaterials*, vol. 35, pp. 3903-3917, 2014.
- [8] L. Ma, C. Gao, Z. Mao, J. Zhou, J. Shen, X. Hu, *et al.*, "Collagen/chitosan porous scaffolds with improved biostability for skin tissue engineering," *Biomaterials*, vol. 24, pp. 4833-4841, 2003.
- [9] X. Wang, P. Wu, X. Hu, C. You, R. Guo, H. Shi, *et al.*, "Polyurethane membrane/knitted mesh-reinforced collagen-chitosan bilayer dermal substitute for the repair of full-thickness skin defects via a two-step procedure," *Journal of the mechanical behavior of biomedical materials*, vol. 56, pp. 120-133, 2016.
- [10] G. Lu, B. Sheng, Y. Wei, G. Wang, L. Zhang, Q. Ao, *et al.*, "Collagen nanofiber-covered porous biodegradable carboxymethyl chitosan microcarriers for tissue engineering cartilage," *European Polymer Journal*, vol. 44, pp. 2820-2829, 9// 2008.
- [11] S. Yu, X. Zhang, G. Tan, L. Tian, D. Liu, Y. Liu, *et al.*, "A novel pH-induced thermosensitive hydrogel composed of carboxymethyl chitosan and poloxamer cross-linked by glutaraldehyde for ophthalmic drug delivery," *Carbohydrate Polymers*, vol. 155, pp. 208-217, 1/2/ 2017.
- [12] A. Revzin, R. J. Russell, V. K. Yadavalli, W.-G. Koh, C. Deister, D. D. Hile, *et al.*, "Fabrication of poly (ethylene glycol) hydrogel microstructures using photolithography," *Langmuir*, vol. 17, pp. 5440-5447, 2001.
- [13] M. Zhang, X. H. Li, Y. D. Gong, N. M. Zhao, and X. F. Zhang, "Properties and

- biocompatibility of chitosan films modified by blending with PEG," *Biomaterials*, vol. 23, pp. 2641-2648, 7// 2002.
- [14] K. Knop, R. Hoogenboom, D. Fischer, and U. S. Schubert, "Poly (ethylene glycol) in drug delivery: pros and cons as well as potential alternatives," *Angewandte Chemie International Edition*, vol. 49, pp. 6288-6308, 2010.
- [15] G. D. Nicodemus and S. J. Bryant, "Cell encapsulation in biodegradable hydrogels for tissue engineering applications," *Tissue Engineering Part B: Reviews*, vol. 14, pp. 149-165, 2008.
- [16] J. Elisseeff, W. McIntosh, K. Anseth, S. Riley, P. Ragan, and R. Langer, "Photoencapsulation of chondrocytes in poly (ethylene oxide)-based semi-interpenetrating networks," *Journal of biomedical materials research*, vol. 51, pp. 164-171, 2000.
- [17] S. J. Bryant and K. S. Anseth, "Controlling the spatial distribution of ECM components in degradable PEG hydrogels for tissue engineering cartilage," *Journal of biomedical materials research Part A*, vol. 64, pp. 70-79, 2003.
- [18] K. L. Spiller, S. A. Maher, and A. M. Lowman, "Hydrogels for the repair of articular cartilage defects," *Tissue engineering part B: reviews*, vol. 17, pp. 281-299, 2011.
- [19] C. G. Williams, T. K. Kim, A. Taboas, A. Malik, P. Manson, and J. Elisseeff, "In vitro chondrogenesis of bone marrow-derived mesenchymal stem cells in a photopolymerizing hydrogel," *Tissue engineering*, vol. 9, pp. 679-688, 2003.
- [20] Y. F. Poon, Y. Cao, Y. Liu, V. Chan, and M. B. Chan-Park, "Hydrogels based on dual curable chitosan-graft-polyethylene glycol-graft-methacrylate: application to layer-by-layer cell encapsulation," *ACS applied materials & interfaces*, vol. 2, pp. 2012-2025, 2010.
- [21] E. Bakaic, N. M. Smeets, and T. Hoare, "Injectable hydrogels based on poly (ethylene glycol) and derivatives as functional biomaterials," *RSC Advances*, vol. 5, pp. 35469-35486, 2015.
- [22] S. P. Zustiak and J. B. Leach, "Hydrolytically degradable poly (ethylene glycol) hydrogel scaffolds with tunable degradation and mechanical properties," *Biomacromolecules*, vol. 11, pp. 1348-1357, 2010.
- [23] T. Buranachai, N. Praphairaksit, and N. Muangsin, "Chitosan/polyethylene glycol beads crosslinked with tripolyphosphate and glutaraldehyde for gastrointestinal drug delivery," *Aaps Pharmscitech*, vol. 11, pp. 1128-1137, 2010.
- [24] X. Fernández-Francos and X. Ramis, "Structural analysis of the curing of epoxy thermosets crosslinked with hyperbranched poly(ethyleneimine)s," *European Polymer Journal*, vol. 70, pp. 286-305, 9// 2015.
- [25] R. Sabater i Serra, A. Kyritsis, J. Escobar Ivirico, A. Andrio Balado, J. Gómez Ribelles, P. Pissis, *et al.*, "Structure and dynamics in poly(L-lactide) copolymer networks," *Colloid and Polymer Science*, vol. 288, pp. 555-565, 2010/03/01 2010.
- [26] N. Vasylieva, B. Barnych, A. Meiller, C. Maucler, L. Pollegioni, J.-S. Lin, *et al.*, "Covalent enzyme immobilization by poly (ethylene glycol) diglycidyl ether (PEGDE) for microelectrode biosensor preparation," *Biosensors and Bioelectronics*, vol. 26, pp. 3993-4000, 2011.
- [27] R. Pauliukaite, M. E. Ghica, O. Fatibello-Filho, and C. M. Brett, "Comparative study of different cross-linking agents for the immobilization of functionalized carbon nanotubes within a chitosan film supported on a graphite- epoxy composite electrode," *Analytical chemistry*, vol. 81, pp. 5364-5372, 2009.
- [28] H.-C. Ge and D.-K. Luo, "Preparation of carboxymethyl chitosan in aqueous solution under microwave irradiation," *Carbohydrate research*, vol. 340, pp.

- 1351-1356, 2005.
- [29] A. Svärd, E. Brännvall, and U. Edlund, "Rapeseed straw as a renewable source of hemicelluloses: Extraction, characterization and film formation," *Carbohydrate Polymers*, vol. 133, pp. 179-186, 11/20/ 2015.
- [30] M. A. Gámiz-González, P. Guldreis, C. M. Antolinos Turpín, J. Ródenas Rochina, A. Vidaurre, and J. L. Gómez Ribelles, "Fast degrading polymer networks based on carboxymethyl chitosan," *Materials Today Communications*, vol. 10, pp. 54-66, 3// 2017.
- [31] B. Satheesh, K. Tshai, and N. Warrior, "Effect of Chitosan Loading on the Morphological, Thermal, and Mechanical Properties of Diglycidyl Ether of Bisphenol A/Hexamethylenediamine Epoxy System," *Journal of Composites*, vol. 2014, 2014.
- [32] M. N. V. Ravi Kumar, "A review of chitin and chitosan applications," *Reactive and Functional Polymers*, vol. 46, pp. 1-27, 11// 2000.
- [33] W. Zhao, L. Glavas, K. Odelius, U. Edlund, and A.-C. Albertsson, "Facile and Green Approach towards Electrically Conductive Hemicellulose Hydrogels with Tunable Conductivity and Swelling Behavior," *Chemistry of Materials*, vol. 26, pp. 4265-4273, 2014/07/22 2014.
- [34] H. Kono, "Characterization and properties of carboxymethyl cellulose hydrogels crosslinked by polyethylene glycol," *Carbohydrate polymers*, vol. 106, pp. 84-93, 2014.
- [35] I. Aranaz, R. Harris, and A. Heras, "Chitosan amphiphilic derivatives. Chemistry and applications," *Current Organic Chemistry*, vol. 14, p. 308, 2010.
- [36] M. Rinaudo, P. Le Dung, C. Gey, and M. Milas, "Substituent distribution on O, N-carboxymethylchitosans by  $^1\text{H}$  and  $^{13}\text{C}$  NMR," *International journal of biological macromolecules*, vol. 14, pp. 122-128, 1992.
- [37] S. Jabeen, S. Saeed, A. Kausar, B. Muhammad, S. Gul, and M. Farooq, "Influence of Chitosan and Epoxy Cross Linking on Physical Properties of Binary Blends," *International Journal of Polymer Analysis and Characterization*, 2015.
- [38] M. E. S. Miranda, C. Marcolla, C. A. Rodrigues, H. M. Wilhelm, M. R. Sierakowski, T. M. B. Bresolin, *et al.*, "Chitosan and N-carboxymethylchitosan: I. The role of N-carboxymethylation of chitosan in the thermal stability and dynamic mechanical properties of its films," *Polymer International*, vol. 55, pp. 961-969, 2006.
- [39] L. Gao, H. Gan, Z. Meng, R. Gu, Z. Wu, L. Zhang, *et al.*, "Effects of genipin cross-linking of chitosan hydrogels on cellular adhesion and viability," *Colloids and Surfaces B: Biointerfaces*, vol. 117, pp. 398-405, 5/1/ 2014.
- [40] T. Zhang, J. Chen, Q. Zhang, J. Dou, and N. Gu, "Poly (ethylene glycol)-cross linked poly (methyl vinyl ether-co-maleic acid) hydrogels for three-dimensional human ovarian cancer cell culture," *Colloids and Surfaces A: Physicochemical and Engineering Aspects*, vol. 422, pp. 81-89, 2013.
- [41] H. Tan, C. R. Chu, K. A. Payne, and K. G. Marra, "Injectable in situ forming biodegradable chitosan-hyaluronic acid based hydrogels for cartilage tissue engineering," *Biomaterials*, vol. 30, pp. 2499-2506, 2009.
- [42] M. Browning, S. Cereceres, P. Luong, and E. Cosgriff-Hernandez, "Determination of the in vivo degradation mechanism of PEGDA hydrogels," *Journal of Biomedical Materials Research Part A*, vol. 102, pp. 4244-4251, 2014.
- [43] G. Lu, L. Kong, B. Sheng, G. Wang, Y. Gong, and X. Zhang, "Degradation of covalently cross-linked carboxymethyl chitosan and its potential application for peripheral nerve regeneration," *European Polymer Journal*, vol. 43, pp. 3807-

3818, 2007.

- [44] P. J. Flory, "Network Structure and the Elastic Properties of Vulcanized Rubber," *Chemical reviews*, vol. 35, pp. 51-75, 1944.